Eur. Phys. J. D **40**, 417–422 (2006)
DOI: 10.1140/epjd/e2006-00160-9

THE EUROPEAN PHYSICAL JOURNAL D

Multiple Devil's staircase in a discontinuous circle map

X.-M. Wang[1,a], Z.-J. Fang[2], and J.-F. Zhang[1]

[1] School of Physics and Electric Information, NingXia University, Yinchuan 750021, P.R. China
[2] School of Sciences, HeBei University of Technology, Tianjin 300130, P.R. China

Received 6 February 2006 / Received in final form 15 May 2006
Published online 12 July 2006 –

Abstract. The multiple Devil's staircase, which describes phase-locking behavior, is observed in a discontinuous nonlinear circle map. Phase-locked steps form many towers with similar structure in winding number(W)-parameter(k) space. Each step belongs to a certain period-adding sequence that exists in a smooth curve. The Collision modes that determine steps and the sequence of mode transformations create a variety of tower structures and their particular characteristics. Numerical results suggest a scaling law for the width of phase-locked steps in the period-adding ($W = n/(n+i)$, $n, i \in int$) sequences, that is, $\Delta k(n) \propto n^{-\tau}$ ($\tau > 0$). And the study indicates that the multiple Devil's staircase may be common in a class of discontinuous circle maps.

PACS. 05.45.Ac Low-dimensional chaos

1 Introduction

Phase locking behavior is one of the basic characteristics of nonlinear systems, and exists in many physical systems [1–4]. The most famous is the one-dimensional map of the circle onto itself, called "circle map". In such a map the winding number $W(\epsilon)$ is defined by the mean number of rotations per iteration. It is locked onto every single rational value to form a curve consisting of an infinite number of steps when the control parameter ϵ varies. The curve is called a Devil's staircase. Its beautiful self-similar structure attracted much attention in 1980's and therefore had experimental or numerical proofs in quite different contexts. For instance, the typical examples are presented in the references [5,6]. The Devil's staircase shows two basic features: the distribution of the phase-locked steps demonstrates monotonicity and self-similarity that can be fully described by the Farey tree rule. It means: if there are two winding numbers, $W = M/s$ and $W' = M'/s'$ ($M, M', s, s' \in int$), which are phase locked in $\Delta\epsilon$ and $\Delta\epsilon'$, then the winding number of the largest phase locking interval (or say phase-locked step) between $\Delta\epsilon$ and $\Delta\epsilon'$ is $W = (M + M')/(s + s')$. In 1997, references [7,8] reported the so-called multiple Devil's staircase (MDS) observed in a piecewise continuous linear circle map with two discontinuous regions. This Devil's staircase, in comparison with the conventional Devil's staircase (CDS), loses monotonicity and self-similarity, and is composed of many tower-like structures. Each tower includes two branches. Some of these branches are CDSs. The top steps and the bottom steps of all towers are located in two smooth curves, and the other points are confined between these two curves.

In fact, all of the top steps of the towers belong to a period-adding sequence with winding number, $W = n/(n+2)$ ($n \in int$), while the bottom steps form another period-adding sequence with W of $n/(n+3)$ ($n \in int$). The widths of such steps obey a general scaling law, $\ln|\Delta\varepsilon(n)| \propto n$, when $n \to \infty$ [9]. Here $\Delta\varepsilon(n)$ denotes the width of the step with $W(n)$. As stated by Kaneko [10], the reasons for the choice of the steps is that the sequence can be observed since it has a large stable region and that it reveals the global property of lockings through various scalings. So the scaling law is basic for the phase-locking.

The authors of references [7,8] pointed out that the mechanism inducing the MDS is the so-called multiple collision modes. Each mode is expressed by a pair of discontinuous points, say the left and the right points, and thus there are 4 modes in this system. A stable periodic point collides the left point with the parameter value at the left end point of a phase-locked step, while it collides the right point with the parameter value at the right end point of the step. References [11,12] stated that there are in total 16 following ways, which represent the modes after each mode. They can serve as basic units that generate the branches of the towers. And two of them can create two CDS branches, the ascendant and descendant, to form a full tower so that each period-adding sequence can find their step on the branches, while the other ways can induce the steps to form a fragmentary tower, and thus the steps that should belong to some period-adding sequences are absent. The former was named after the sonant structure and the latter the dissonant structure. Reference [12]

[a] e-mail: wxmwang@nxu.edu.cn

also studied how the structure develops when the number of the discontinuous regions increases and suggested a concept, dissonance of MDS, to quantitatively describe this development.

In other words, the structure of the tower is determined by the way the mode transformations move from one to another to produce steps one by one. So a given sequence of mode transformations determines a particular tower structure. However, one may have the question: whether the MDS is a special phenomenon in the aforementioned system or a general feature of a class of systems? This may be important and interesting. The results that will be presented in this article show that systems do not necessarily have to be piecewise linear to generate multiple collision modes and demonstrate MDSs, and the most likely general sort of such systems is a circle map, linear or nonlinear.

2 Discontinuous nonlinear circle map

It is well-known that the circle map is an very important nonlinear model, which can exhibit many dynamical behaviors such as CDSs for describing phase-lockings, the route to chaos via the transformation from quasiperiodicity and the corresponding scaling properties and so on. And it can describe many physical systems, for instance, current-driven Josephson junctions [6] and driven charge-density-wave systems [13]. The typical circle map is

$$\theta_{n+1} = \varphi(\theta_n) = \theta_n + \Omega - \frac{k}{2\pi}\sin(2\pi\theta_n) \qquad [mod.\ 1]. \quad (1)$$

We can obtain the studied general circle map by introducing the discontinuity to the above model, i.e.,

$$\theta_{n+1} = \begin{cases} \varphi_1(\theta_n) = \theta_n + \Omega - \dfrac{k}{2\pi}\sin(2\pi\theta_n) + D_{01}, \\ \qquad\qquad\qquad\qquad \theta_n \in [0, \theta_B], \\ \varphi_2(\theta_n) = \theta_n + \Omega - \dfrac{k}{2\pi}\sin(2\pi\theta_n) - 0.5 - D_{02}, \\ \qquad\qquad\qquad\qquad \theta_n \in (\theta_B, \theta_E), \\ \varphi_3(\theta_n) = A * \theta_n + \Omega - \dfrac{k}{2\pi}\sin(2\pi\theta_n) - D_{03}, \\ \qquad\qquad\qquad\qquad \theta_n \in [\theta_B, 1]. \end{cases} \quad (2)$$

The locations of the branches of the function are shown in Figure 1. φ_3 multiplied by A of which value is less than one is needed to form a channel, with the diagonal, for the periodic orbits. The exit of the channel is denoted by the point, $\theta_E(\theta_E = \varphi^{-1}(1))$. G represents the implied discontinuous point that divides the exit into two equal parts. Its left and right limit definition is $\theta_{G^-} = \varphi_2^{-1}(\varphi_1^{-1}(\theta_B))$ and $\theta_{G^+} = \varphi_2^{-2}(\theta_C)$, respectively. And the coordinates of the other points are determined by the equations, $\varphi_2(\varphi_2(\theta_{D_1})) = 0$, $\theta_B = \theta_C = \varphi_2(\theta(D_1))$, $D_{01} = 1 - \varphi(\theta_C)$, $\varphi_3(\theta_E) = 0.5$. k denotes the strength of the driving force in many systems, including this model, and is chosen as the control parameter.

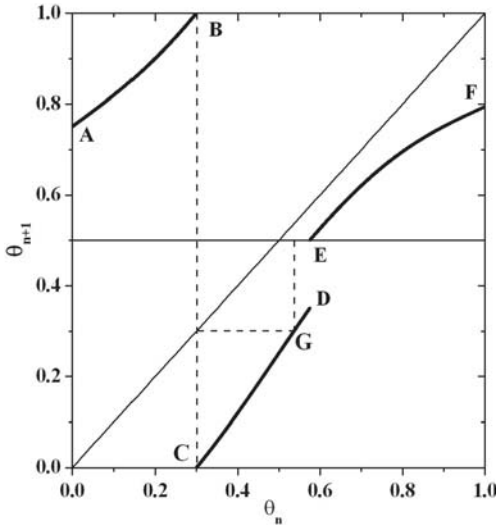

Fig. 1. A schematic drawing of map 1. The solid curves denote the mapping function. The dashed lines show point G is the second backward images of both the discontinuous points B and C, and thus is a implicit discontinuous point to divide the exit of the channel into two equal parts.

The border-collision bifurcation is one of the basic dynamic behaviors in discontinuous systems [14,15]. It indicates, since the discontinuous points of the mapping functions are non-differentiable, an orbit that visits (collides) such points will lose its stability and be replaced by a new stable one. In this case, it is very possible that the system is locked in a series of periodic states as a parameter is varied. These phase-locked regions manifest as a series of phase-locked steps in the winding number-parameter space. The winding number can be defined as the proportion of the iteration number, $N_c^{'}$, inside the channel to the total iteration number, $N_t^{'}$, of the trajectory. That is,

$$W = \lim_{N_t^{'} \to \infty} \frac{N_c^{'}}{N_t^{'}}. \quad (3)$$

For a periodic orbit, it also can, at first hand, be expressed as

$$W = \frac{N_c}{N_t}. \quad (4)$$

The denotations of N_c and N_t are the same of $N_c^{'}$ and $N_t^{'}$. In this article we choose the constant parameters, $\Omega = 0.4$. As A takes different values the structures of the MDSs are likely to be different. In order to get more understanding on the detailed mechanism of the MDS, we first choose $A = 0.75$ where the MDS demonstrates sonant structure, and present the investigations in the next section, Section 3. Some of the conclusions can be extended to the dissonant structure, and will be presented in Section 4.

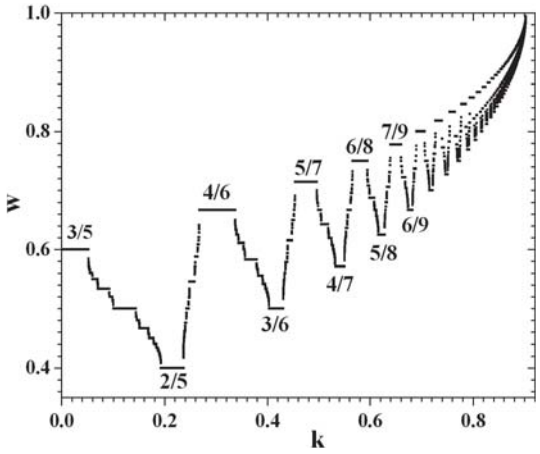

Fig. 2. The sonant MDS obtained numerically by the definition (4) in map (1). The first 3000 iterations are dropped to avoid transience.

3 Sonant structures of the multiple Devil's staircase

3.1 Features of the multiple Devil's staircase

Figure 2 shows the sonant MDS obtained numerically by equation (4). The contour of the MDS is, as a whole, similar to those previously reported. The phase-locked steps are regularly arranged in smooth curves, that is, theoretically speaking, there are infinity number of period-adding sequences that confine the phase-lockings. The features of the MDS can be summed up as followings: (1) it is composed of many full towers with similar structure. (2) Each tower includes two branches that are CDSs. (3) All the phase-locked steps are confined by two smooth curves, which contain the top and bottom steps, respectively. (4) The total iteration number, N_t, of the trajectory corresponding to the top step is equal to that of the right bottom step in the same tower. Reference [7] revealed that there are 4 collision modes in the linear discontinuous circle map. The analytical result in reference [11] showed that there are only 4 collision modes and obtained the conditions, which are proved to be associated with the following modes that correspond to the transformations between the neighbor steps. Since the present observations only described the sonant structure, we focus on the mechanisms that cause the steps to be confined by two smooth curves, the origin of the similar structure of the towers and the scaling law for the period-adding sequences. In fact, the analyses may easily be conducted in this case.

The very careful studies show that there are 4 collision modes in the direction of the control parameter k increasing. They can be described by the discontinuous points of the map with which the periodic orbits will collide: $1(G^-, E)$, $2(D, E)$, $3(G^-, G^+)$ and $4(D, G^+)$. The transformations of the collision modes are arranged in such a perfect way that the tower structure repeats regularly as follows: $\cdots 1(\mathrm{TS}) \rightarrow 2(\mathrm{DS}) \cdots 2 \rightarrow 4(\mathrm{BS}) \rightarrow 3(\mathrm{AS}) \cdots 3 \rightarrow \cdots$. Here the characters TS, BS, DS and AS represents the top step, bottom step, the step in the descendant branch and that in the ascendant branch, respectively. This array indicates that mode 1 determines the top steps, mode 2 generates all of the steps in the descendant branches, mode 3 generates all of steps in the ascendant branches and mode 4 generates the bottom steps.

In order to more conveniently discuss the details of the structure of the MDS, we use the definition of the winding number suggested in references [5,6]. That is,

$$W(L, l; R, r) = \frac{L + R}{L + R + 2l + 3r}, \tag{5}$$

where l is the number of re-injection via the left part of the exit in a periodic trajectory, and r is that via the right part of the exit. And 2 represents the iteration number outside the channel of a periodic trajectory before each re-injection via the left part of the exit, and 3 represents that via the right part of the exit. $L = \sum_{i=1}^{l} L_i$, $R = \sum_{j=1}^{r} R_j$, where L_i denotes the iteration number inside the channel after ith re-injection via the left part of the exit, and R_j denotes that after jth re-injection via the right part of the exit. Then a phase-locked step can be represented by four characters, $(L, l; R, r)$. $(L, 1; 0, 0)$ denotes a TS, $(0, 0; R, r)$ denotes a BS and $(L, l \neq 0; R, r \neq 0)$ denotes a AS or a DS. Since one period-adding sequence differ from another only in the value of l or r a period-adding sequence can be denoted by two characters, $(l : r)$. Based on this definition some important understandings or conclusions will be obtained.

(1) All the TSs belong to the period-adding-1 sequence, $(1 : 0)$, with winding number $W = L/(L + 2)$. All of the BSs belong to the period-adding-1 sequence, $(0 : 1)$, with winding number $W = R/(R + 3)$. Some ASs and DSs belong to the sequences period-adding-t_1, $(l \geq 1 : r \geq 1)$, where $t_1 \leq l, r$. The period-adding of the former can be performed only via L, and that of the latter can be performed only via R. The other ASs and DSs belong to the sequences period-adding-t_2, $(l \geq 1 : r \geq 1)$, and the period-adding can be performed via both of L and R. Where $t_2 \leq l + r$. For instance, the middle steps in the ascendant branches or in the descendant branches respectively belong to two different period-adding-2 sequences. Here a middle step is the longest step except the TS and the BS in a branch, and 2 is due to $l + r = 2$. Therefore, all of the steps belong to one sequence should located consequentially in one smooth curve.

(2) As shown by numerical investigations, the TS and the right BS (bottom end step of the descendant branch) of each tower correspond to two orbits with the same number of period-points, i.e., $N_t = L + 2 = R + 3$, so we have $L = R + 1$ for the two steps in one tower. For an arbitrary step determined by mode 2 in the descendant branch, the winding number can be easily and reasonably approximated as

$$W(L', l; R', r) \doteq \frac{lL + rR}{lL + rR + 2l + 3r}. \tag{6}$$

From the right hand side of the equation, we can easily obtain the following equations

$$\frac{lL+rR}{lL+rR+2l+3r} = \frac{L}{L+2} - \frac{r}{(l+r)(L+2)} \quad (7)$$

and

$$\frac{lL+rR}{lL+rR+2l+3r} = \frac{R}{R+3} + \frac{l}{(l+r)(R+3)}. \quad (8)$$

For $l, r \geq 1$, one may have, by comparing equations (7) with (8), $W(L,1;0,0) > W(L^{'},l;R^{'},r) > W(0,0;R,1)$. It indicates that all of the steps are confined between two sequences composed of TSs and BSs, respectively.

(3) When the parameter varies in the direction of k increasing, the sequence of the mode transformations reads $1 \to 2\cdots2 \to 4 \to 3\cdots3\cdots$, the corresponding phase-locked steps extend along the route: descending-ascending-descending-ascending... to form a series of the towers. These towers show the similar structures due to the fact that each step in the tower belongs to the corresponding period-adding sequence.

(4) For a certain sequence (the values of l and r are fixed), one may have $W(L^{'},l;R^{'},r) \to W(L,1;0,0)$ and $W(L^{'},l;R^{'},r) \to W(0,0;R,1)$ when the parameter, k, increases, and $L, R \to \infty$ meanwhile. Therefor, there should be the relation, $W(0,0;R,1) = W(L,1;0,0) \to 1$. It implies that the steps in all of sequences will be compressed in the $W-$axis, and finally lead to the overlapping of the sequence $(1:0)$ and $(0:1)$, which agrees with what we observed in Figure 2.

3.2 Scaling properties of the period-adding sequences

As it has already discussed above, in the direction of k increasing, the steps distribute in the special ways to form the period-adding sequences and show some special scaling properties. In this article three important results for sequences $(1:0)$, $(0:1)$ and $(1:1)$ are presented.

For $(1:0)$: the width of each step can be theoretically obtained from the collision conditions at its end parameter. According to collision conditions determined by mode 1, that is, $\varphi_3^{(L)}\varphi_1\varphi_2(\theta_{G^-})|_{k=k_L^s} = \theta_{G^-}$ and $\varphi_3^{(L)}\varphi_1\varphi_2(\theta_E)|_{k=k_L^e} = \theta_E$, we have $\Delta k(n) = k_L^e - k_L^s, n = L+2$. The scaling property can be derived as $n \to \infty$. It is very hard to give this expression in analytic form due to the nonlinearity of mapping function. So are the other sequences. However, the numerical results can be obtained easily. As showed in Figure 3a, the linear fitted line in $\ln \Delta k - \ln n$ space suggests a scaling law $\Delta k(n) \propto n^{\alpha}$, $\alpha = -2.840 \pm 0.006$.

For $(0:1)$: as shown by Figure 3b, a similar procedure gives the scaling law, $\Delta k(n) \propto n^{\beta}$, $\beta = -2.848 \pm 0.014$, $n = R+3$.

For $(1:1)$: it actually includes two sequences. One is composed of the middle steps in the ascendant branches, and the other is composed of the middle steps in the descendant branches. As showed in Figure 3c, the result indicated by circles and their fitted line presents the scaling property, $\Delta k(n) \propto n^{\gamma_A}$, $\gamma_A = -4.318 \pm 0.049$, for ascendant branch $(1:1)$ sequence. The similar result for the descendant branch $(1:1)$ sequence, $\Delta k(n) \propto n^{\gamma_B}$, $\gamma_B = -1.979 \pm 0.022$, is also showed in Figure 3c with

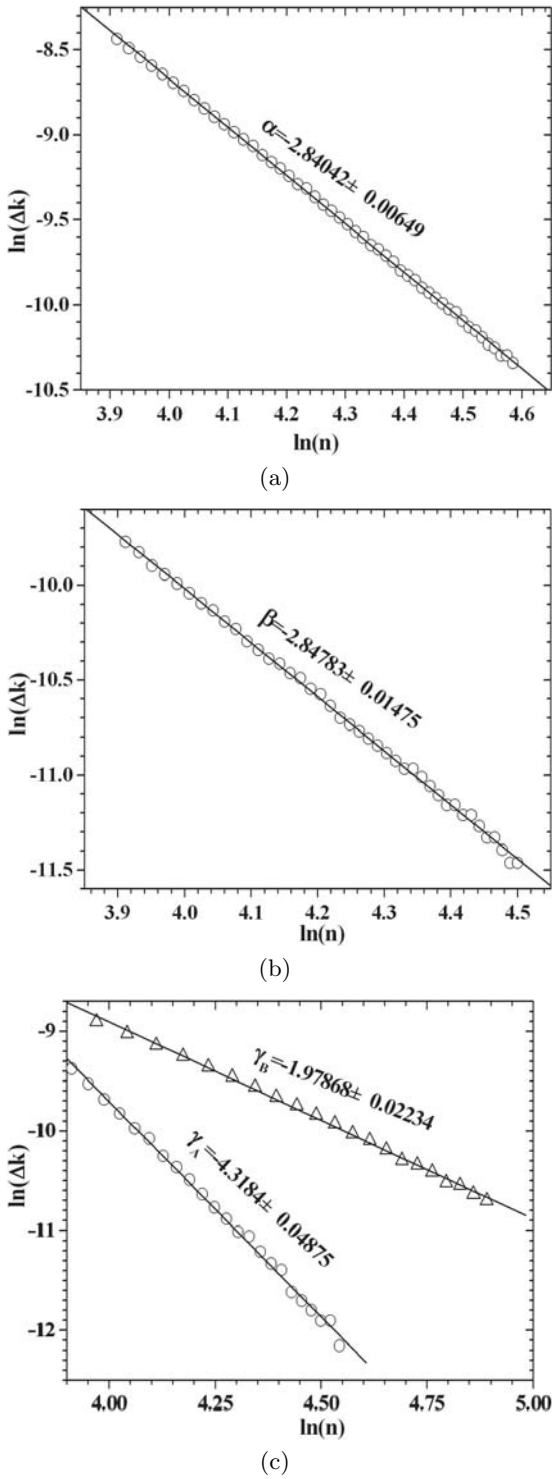

Fig. 3. Numerical results about the scaling properties (a) for sequence $(1:0)$, (b) for sequence $(0:1)$, and (c) for two sequences $(1:1)$. The details are presented in the text.

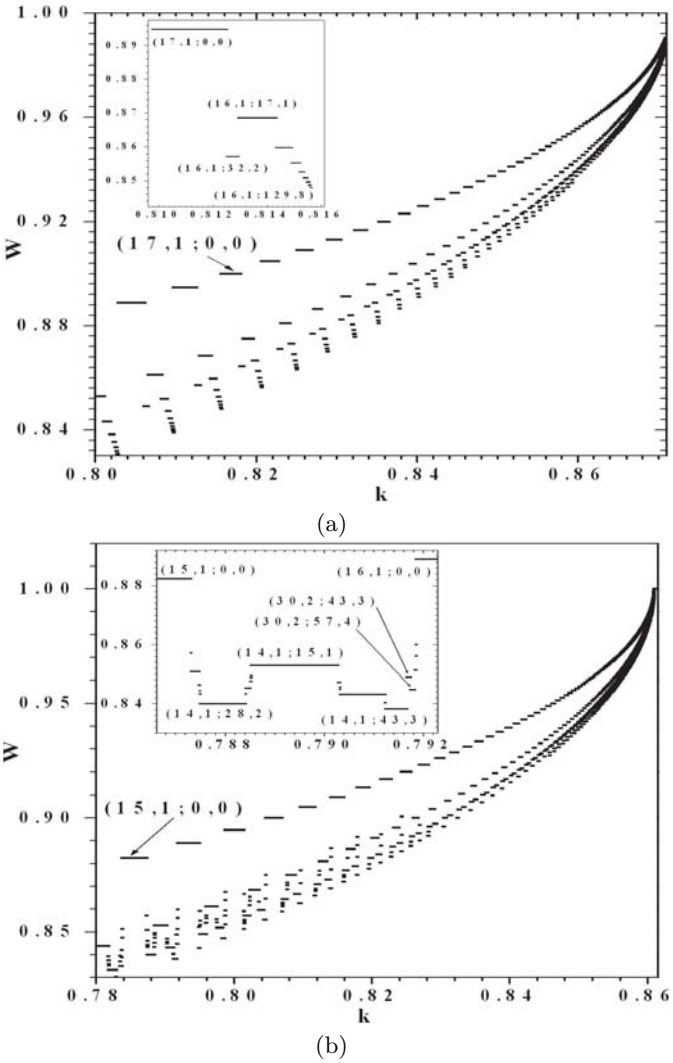

Fig. 4. The dissonant MDSs computed with the parameter value (a) $A = 7.8$ and (b) $A = 7.9$, respectively. Both the insets of (a) and (b) are the partial magnifications. And the first 3000 iterations are dropped to avoid transience for all computations.

triangles. Please note here $n = L+2+R+3$ gives the periodic points of the corresponding periodic orbit. The similar results obtained in the other sequences ($l \geq 1 : r \geq 1$) convince us that the scaling law

$$\Delta k(n) \propto n^{-\tau},\ \tau > 0, \tag{9}$$

is common to all of the period-adding sequences in this map.

4 Dissonant structures of the multiple Devil's staircase

As stated in the last section, the sequence of the mode transformations determine the structure of the MDS. In order to get a general picture of the MDS and its dissonant structure, we present the main ideas here. In this discontinuous circle map, there are only two possible following modes after each mode: $1 \to 2$ or 4, $2 \to 2$ or 4, $3 \to 3$ or 1, $4 \to 3$ or 1, which are the basic units to generate the branches of the tower, and thus their arrangements in different order will lead to different tower structure. Please note that there is no preference for mode 1 and 4 to just confine the steps $(L, 1; 0, 0)$ or $(0, 0; R, r)$. They can also induce the steps $(L, l \geq 1; R, r \geq 1)$ that can serve as the top and bottom steps. So mode 1 and mode 4 can respectively be classified into the single-exit one ($W(L, 1; 0, 0)$ or $W(0, 0; R, 1)$ which indicates that the orbit escapes the exit of the channel via only single part, the left or the right) and the multiple-exit one ($W(L, l \geq 1; R, r \geq 1)$ which means the orbit escapes the exit via both of the parts of the exit). The former can be denoted by the character s, and the latter can be denoted by the character m. So we can use the words "mode $1s$" or "mode $1m$" and "mode $4s$" or "mode $4m$" in our discussions. And therefore, there are 16 basic units. These results are proved by our numerical simulations to be correct and in good agreements with what presented in references [9,11] obtained analytically and numerically. Thus the sequence of the mode transformations by which the sonant tower structure repeats perfectly in Figure 2 can be expressed more accurately as: $\cdots 1s \to 2\cdots 2 \to 4s \to 3\cdots 3\cdots$.

As two typical examples of the dissonant tower structures, which may provide our readers with basic impressions on the features of these structures, are showed in Figure 4. Figure 4a shows a numerically obtained MDS with $A = 0.78$. The value is only a little bit different from those stated in Figure 2. The dissonant tower structure is induced by the mode transformations $\cdots 1s \to 4m \to 1m \to 2\cdots 2 \to 4m\cdots$. The inset is the partial magnification of Figure 4a, which shows many dissonant structure units or the following modes. We list them in turn from the left to the right:

$$\begin{aligned} 1s(17,1;0,0) &\to 4m(16,1;32,2),\\ 4m(16,1;32,2) &\to 1m(16,1;17,1),\\ 1m(14,1;15,1) &\to 2\cdots 2 \to 4m(14,1;17,1),\\ 1m(16,1;17,1) &\to 2\cdots 2 \to 4m(16,1;129,8). \end{aligned}$$

And is followed by $4m(16,1;129,8) \to 1s(18,1;0,0)$. Figure 4b shows another example with $A = 0.79$. The mode transformations follow $\cdots 1s \to 2\cdots 2 \to 4m \to 3\cdots 3 \to 1m \to 2\cdots 2 \to 4m \to 1m \to 4m \to 3\cdots 3\cdots$. Similarly, we only present the details of the inset. The structure units are

$$\begin{aligned} 1s(15,1;0,0) &\to 2\cdots 2 \to 4m(14,1;28,2),\\ 4m(14,1;28,2) &\to 3\cdots 3 \to 1m(14,1;15,1),\\ 1m(14,1;15,1) &\to 2\cdots 2 \to 4m(14,1;43,3),\\ 4m(14,1;43,3) &\to 1m(30,2;43,3),\\ 1m(30,2;43,3) &\to 4m(30,2;57,4). \end{aligned}$$

The rest of the dissonant structure units can be obtained by varying the parameter properly.

Someone may wonder whether the width scaling properties, which dominates the distribution of the phase-locked steps in sonant MDSs, apply to these dissonant ones? The numerical investigations show that the distribution of the steps obeys the same scaling law that the distribution of the steps in the sonant MDSs does, $\Delta k(n) \propto n^{-\tau}(\tau > 0)$, which has been presented in the last section. For instance, as showed by the inset of Figure 4a, the step $(16, 1; 32, 2)$ and the steps that are located in the same positions of the similar towers belong to the period-adding-3 sequence with $W = n/(n + 9)$. The step $(16, 1; 129, 8)$ and the steps that are located in the corresponding positions of the similar towers belong to the period-adding-9 sequence with $W = n/(n + 26)$. And thus we can obtain the conclusion that the steps both in the sonant and dissonant MDS are all confined by two smooth curves on which the steps are induced by modes $1s$ or $1m$, and $4s$ or $4m$. Therefore, the similar conclusions obtained in Section 3.1 are valid for the dissonant MDS. However, one may note in the dissonant MDSs, the Farey tree rule doesn't work even for the units induced by the following modes, $1 \to 2\cdots2 \to 4$ or $4 \to 3\cdots3 \to 1$, which often are CDSs. In the inset of Figure 4a, for instance, the step between $(17, 1; 0, 0)$ $(W = 17/19)$ and $(16, 1; 17, 1)$ $(W = 33/38)$, which should have the winding number $W = 50/57$ according to the Farey tree rule, is absent here. As is well-known, this step should belong to the CDS $1s(17, 1; 0, 0) \to 2\cdots2 \to 4m(16, 1; 17, 1)$. These absences may be attributed to the increasing of the nonlinearity of the mapping function branch, φ_3, in map (1) as A increases. Because some periodic orbits, especially the longer ones, have more periodic points to visit on the segment where the slope is more than one, the orbits lose stability, and can not appear.

5 Conclusions and discussions

In this article we present some analytic and numerical investigations on the feature of the multiple Devil's staircase in a discontinuous nonlinear circle map. There are 4 collision modes and 16 possible following modes. 14 of them can induce dissonant tower structures. A given sequence of mode transformations, the regular repetitions of some modes, generate particular and similar towers, and also determine the period-adding sequences in the sonant and dissonant MDSs. These are the same as those that were observed in the previous studied linear maps. However, the smooth curves of the sequences have more complicated function forms other than that $(W \propto -1/\ln(\epsilon), \epsilon$ is the control parameter) in the linear maps. They can be fitted to some polynomials, which may be induced by the nonlinearity of the function.

The width of the phase-locked steps in the period-adding sequences obeys the scaling law, $\Delta k(n) \propto n^{-\tau}$ $(\tau > 0)$, which are common to all of the sequences. And it differs from that in the prevenient studies $\ln|\Delta\epsilon(n)| \propto n$. This difference may be also induced by nonlinear of the mapping function. To sum up, the common characteristics of the multiple Devil's staircases in different systems should be attribute to the same discontinuity of a class of circle maps, while the different dynamical behaviors among these maps can naturally be owed to the differences in the mapping functions.

Our investigations that made in the similarly constructed nonlinear circle maps with three (see the discussions in Ref. [12]) and four discontinuous regions support the conclusion: the MDS and its geometric features may be a common manifestation in a class of discontinuous circle maps whether they are nonlinear or linear.

This study is supported by the National Natural Science Foundation of China under Grant No. 10565002 and Ningxia Advanced Researches Foundation of China under Grant No. 04038. The authors would like to thank Prof. Da-Ren He for the very helpful suggestions and discussions.

References

1. P. Bak, R. Bruinsma, Phys. Rev. Lett. **49**, 249 (1982)
2. T. Gilbert, R.W. Gammon, Int. J. Bifur. Chaos **10**, 155 (2000)
3. S. Lacis, J.C. Bacri, A. Cebes, R. Perzynski, Phys. Rev. E **55**, 2640 (1997)
4. D.-R. He, D.-K. Wang, K.-J. Shi, C.-H. Yang, L.-Y. Chao, J.Y. Zhang, Phys. Lett. A **136**, 363 (1989)
5. W.-J. Yeh, D.-R. He, Y.H. Kao, Phys. Rev. B **31**, 1359 (1985)
6. P. Bak, Phys. Today **39**, 38 (1986)
7. S.-X. Qu, S. Wu, D.-R. He, Phys. Lett. A **231**, 152 (1997)
8. S.-X. Qu, S. Wu, D.-R. He, Phys. Rev. E **57**, 402 (1998)
9. C.-Y. Wu, S.-X. Qu, S. Wu, D.-R. He, Chin. Phys. Lett. **15**, 246 (1998)
10. K. Kaneko, Prog. Theor. Phys. **68**, 669 (1982)
11. X.-M. Wang, J.-S. Mao, S.-X. Qu, Z. Zhou, D.-R. He, Phys. Lett. A **293**, 151 (2002)
12. X.-M. Wang, S.-X. Qu, D.-R. He, Int. J. Bifur. Chaos **15**, 1677 (2005)
13. S. Martin, W. Martienssen, Phys. Rev. Lett. **56**, 1522 (1986)
14. H.E. Nusse, E. Ott, J.A. Yorke, Phys. Rev. E **49**, 1073 (1994)
15. H. Lamba, C.J. Budd, Phys. Rev. E **50**, 84 (1994)